UAH
The University of Alabama in Huntsville

FINAL REPORT

UAH Document No 521134-FR

Subscale Beryllium Mirror Demonstrator Testing Support

Contract Number: H-33241D

By:

James B. Hadaway, PI
Patrick Reardon
Joseph Geary
Bruce Peters

June 29, 2001

1.0 Introduction

This report details the tasks completed by the University of Alabama in Huntsville (UAH) under purchase order H-33241D for the Marshall Space Flight Center (MSFC) between August and December of 2000. This effort was a continuation of work begun by UAH under contracts NAS8-97095, H-30198D, H-30788D, H-31228D, & H-31864D.

UAH had successfully designed, implemented, and checked-out a comprehensive Optical Testing System (OTS) for the XRCF to test both the Sub-scale Beryllium Mirror Demonstrator (SBMD), a 0.5 m f/40 beryllium mirror from Ball Aerospace, and the NGST Mirror System Demonstrators (NMSD's). These mirrors consisted of a 1.6 m f/9.4 thin glass mirror from Composite Optics in which the glass was directly bonded to a composite backplate and a 2 m f/10 thin glass actuated mirror from the University of Arizona. The SBMD had already been tested twice prior to cyro-figuring. After the second test, the mirror was polished to produce the required figure at 35 K (i.e. cryo-figured). Thus, the goal of this third SBMD test was to verify that the cryogenic figure requirements had been met.

UAH was to support the third round testing of the SBMD. This was to include support of planning activities with the mirror manufacturer, installation of the appropriate Wavefront Sensor Pallet, optical testing system operations, and test reporting.

2.0 The SBMD

The SBMD, shown in Fig. 1, is a spherical mirror that is 0.532 m in diameter and has a 20 m radius of curvature. It is made of a light-weighted beryllium (O-30) face-sheet supported by a solid beryllium reaction structure using three titanium bipods. There is also a three-legged titanium mount for a radius of curvature actuator attached to the back of the face-sheet. No actuator was installed during this testing. The mirror face has four mm-sized circular fiducials, one at the center and one each near the edge at 3, 9, & 12 o'clock. This mirror assembly was kinematically mounted to an aluminum interfacing structure during testing. The mirror and interfacing structure were supported by the 5-DOF NGST Mirror Support Structure (NMSS) inside the chamber. The SBMD is required to have a figure error $\leq\lambda/4$ peak-to-valley (PV) and mid-spatial error (surface wavelengths 1-10 cm) $\leq\lambda/10$ PV at 632.8 nm at 35±5 K. The radius of curvature is required to be 20.0±0.1 m at the same temperature.

Figure 1. The SBMD.

3.0 The Optical Testing System

The OTS, shown in Fig. 2, was developed to test the figure and radius of curvature of the NGST Mirror System Demonstrators (NMSD's) and the Sub-scale Beryllium Mirror Demonstrator (SBMD) in the vacuum/cryogenic environment of the X-Ray Calibration Facility (XRCF) at MSFC. The OTS was provided by the University of Alabama in Huntsville. The OTS consists of a WaveScope Shack-Hartmann sensor from Adaptive Optics Associates as the main instrument, a Point Diffraction Interferometer (PDI), a Point Spread Function (PSF) imager, an alignment laser, a Leica Disto Pro distance measurement instrument, and a laser source pallet (632.8 nm wavelength) that is fiber-coupled to the sensor instruments. All of the instruments except the laser source pallet are located on a single breadboard known as the Wavefront Sensor Pallet (WSP). The WSP is located on top of a 5-DOF motion system possessing 150 mm of travel range in any direction with an accuracy of 25 μm. All of this equipment is located in the guide tube of the XRCF during operation. Two PC's are located outside the guide tube to control the instruments.

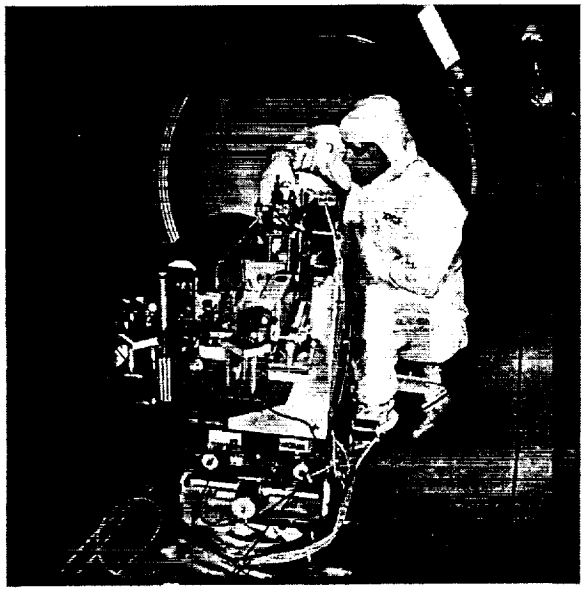

Figure 2. The OTS.

The WaveScope was a special model built for this program. It has four lenslet arrays consisting of 32x32, 50x50, 112x112, & 150x150 subapertures. It also has a 1024x1024 pixel CCD camera with 12 bit resolution and a minimum shutter speed of 0.125 msec. The source fiber has a core diameter of 3.8 μm and an NA of 0.11, presenting an unresolved point-source to the full mirror. The source is located 12 mm off the SBMD's optical axis for the test. The return beam is collimated using an achromatic doublet lens with a focal length of 550 mm. The beam enters the test chamber through a BK7 window (A/R coated) that is 15.875 mm thick, has a clear aperture of 145 mm in diameter, and is tilted 1° in the horizontal direction to prevent retro-reflections from entering the WaveScope. The window is located approximately 610 mm from the WSP with the SBMD center of curvature about 305 mm from the window. While the off-axis source

and tilted window do introduce coma & astigmatism into the measurement, they are only on the order of λ/700 P-V (at 0.6328 μm) in this case.

The error in the figure measurement is dominated by the WaveScope's measurement error in this case. An analysis using a series of reference-to-reference & defocus measurements prior to this test indicated a surface figure error of approximately λ/13 P-V would be attainable in the XRCF environment using the latest measurement procedure. This met both the total & mid-spatial figure requirements for the SBMD with a surface spatial wavelength resolution of 7.3 mm. The error in radius of curvature is dominated by the Leica's absolute measurement error of ±2 mm and the focus setting error (estimated to be ±4 mm). Considering all measurement uncertainties, standard error analysis predicted an overall error in radius of curvature of ±5 mm, easily meeting the requirement of ±100 mm.

The final measurement procedure (NGST Cryogenic Test Bed SBMD Measurement Procedure, MSOP-GS-NGST-414v4) can be examined for further details. A summary is presented below.

- Insure SBMD mirror assembly is thermally stable with a rate less than 2 K/hr and no gradients exceeding 3 K.
- Align WSP to SBMD using both the NMSS 5-DOF & the WSP 5-DOF (includes placing pupil image at same place on CCD every time using mirror fiducials). Best-focus is set mid-way between the two line foci of the astigmatic surface using a shear plate.
- Take reference with fiber source in reference position (facing WaveScope at focus of collimating lens).
- Move fiber to test position (facing mirror, 12 mm off-axis).
- Calibrate using 1/1000 sec exposure time (use circular-variable ND filter on source pallet to set intensity to that of reference) and constant analysis pupil.
- Take a minimum of two measurements (1 single shot & 1 with 7 frames averaged).
- Record PDI fringes & PSF images on thermal printer & to tape.
- Make distance measurement to mirror vertex (after focusing), then to location of mirror's center of curvature on WSP, then take difference between the two along with corrections for window OPL and window-induced focus shift to get radius of curvature.
- Convert OPD data into surface error in correct orientation, save as ASCII, & send to vendor.
- Make CD & tape back-up copies of all data.

4.0 Test Results

Ambient Pressure & Temperature

Measurements in six orientations (60° increments) at ambient pressure & temperature were made on August 22 & 23, 2000. The data was sent to SVG-Tinsley for averaging. The results matched the SVG pre-ship data to within 14 nm rms.

Vacuum & Ambient Temperature

Five independent measurements were made at vacuum and ambient temperature (i.e. the mirror was mis-aligned & realigned to the sensor pallet each time) on August 25 & 26, 2000. In Fig. 3 (next page), the upper plots show the average of the five measurements, followed by the Zernike fit, and then the residual error (difference between raw data and Zernike fit). The Peak-to-Valley (PV) & rms values for each case are given in Table 1. The apparent holes and spikes in the raw data correspond to missing data which the software plots as 0.000 μm. The flat edge of the mirror is at the lower right of the isometric plots.

The cyro corrections are obvious in the average surface and the residual error plots, but do not seem to be as sharp as the original print-through errors (see SBMD 2 residual error in Fig. 4). This was confirmed with the PDI where the triangular corrections were not as distinct as the original errors. The PSF & PDI results are shown in Fig. 5. For SBMD 2, the residual PV was 0.128 μm & the rms was 0.016 μm for the vacuum-ambient case, the PV was 0.169 μm & the rms was 0.022 μm for the vacuum-cryo case, and the PV was 0.134 μm & the rms was 0.016 μm for the cryo-ambient difference. For this test, the average radius of curvature at ambient temperature was 20.015 m.

Measurement	Pressure	Temperature	ROC	PV	rms
VAC/AMB	1.1×10^{-5} Torr	289.2 K	20.015 m	2.979 μm	0.480 μm
Zernike Fit	"	"	N/A	2.521 μm	0.464 μm
Residual	"	"	N/A	0.197 μm	0.026 μm

Table 1. Summary of ambient-average measurement results.

The Zernikes for the average ambient surface are given in Table 2 below. The dominant terms, in order of magnitude, are 0° astigmatism, trefoil (3θ), 45° astigmatism, and a 4θ term. This is the exact order that would be expected from the SBMD 2 data. Also, the magnitudes are very close to what would be expected from the SBMD 2 data (that is, the ambient values plus the negative of the cryo-minus-ambient values). This is shown in Table 3.

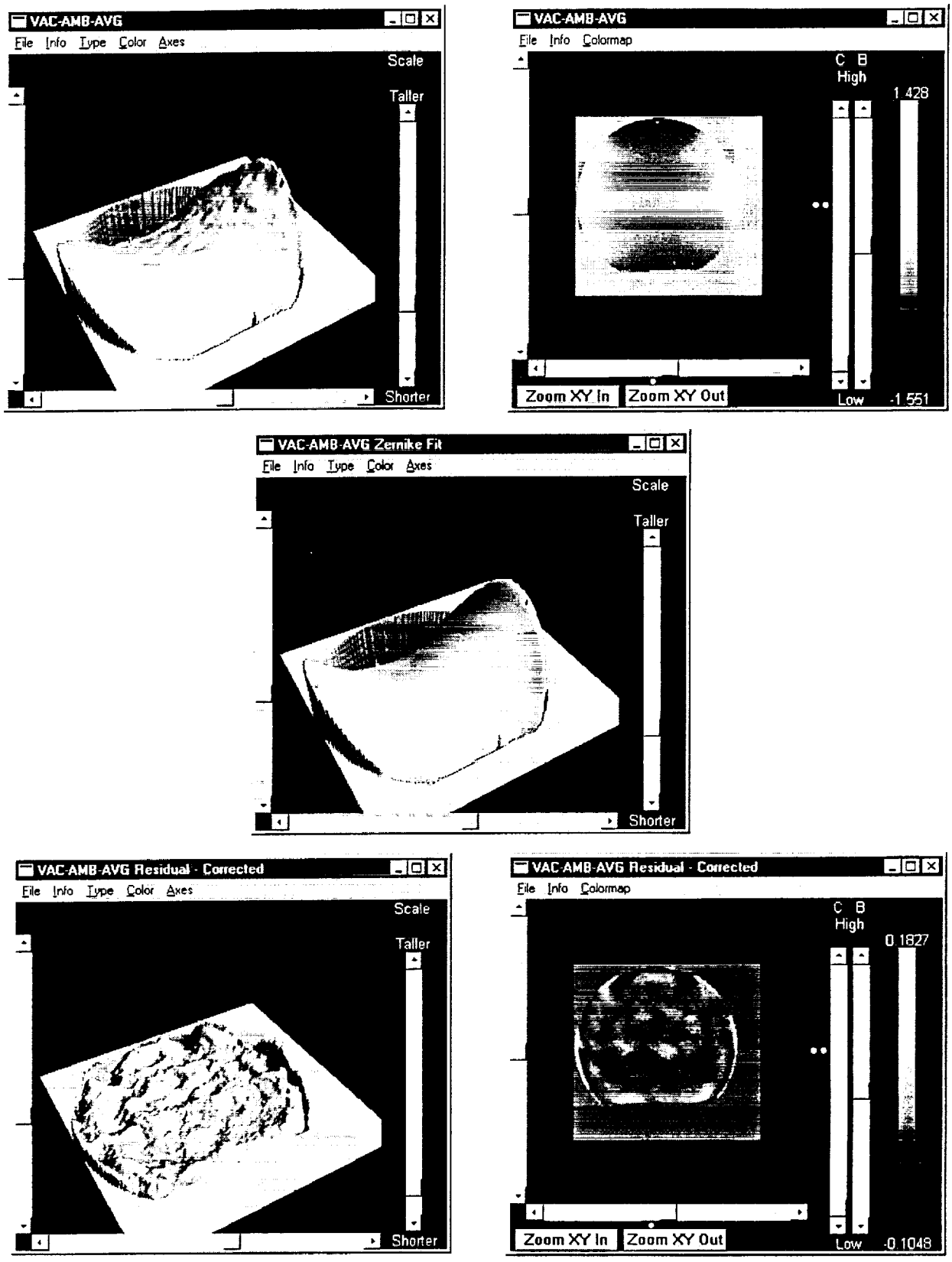

Figure 3. Average ambient surface figure with Zernike decomposition and residual errors.

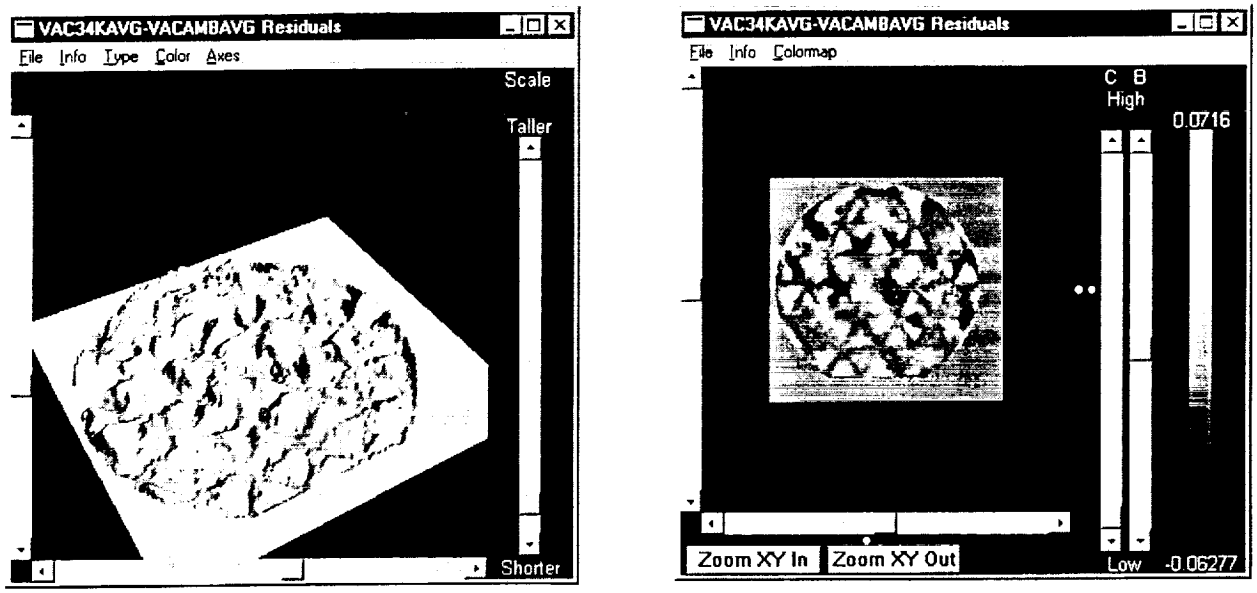

Figure 4. Average ambient residual surface figure error for SBMD 2 cyro-ambient difference.

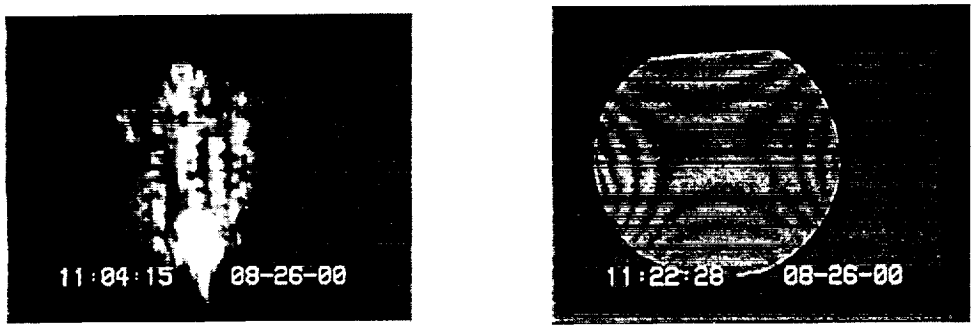

Figure 5. Ambient temperature PSF (left) & PDI (right) results.

Zernike Term (ISO)	AMB, AVG
0 1.0 (Piston)	0.0023979
1 rcos(t) (X Tilt)	0.01621
2 rsin(t) (Y Tilt)	-0.026223
3 $2r^2-1$ (Focus)	0.05801
4 $r^2\cos(2t)$ (0 Astig)	1.0409
5 $r^2\sin(2t)$ (45 Astig)	0.16109
6 $(3r^2-2)r\cos(t)$ (X Coma)	0.01368
7 $(3r^2-2)r\sin(t)$ (Y Coma)	-0.12356
8 $6r^4-6r^2+1$ (Spherical)	0.078967
9 $r^3\cos(3t)$ (Trefoil 1)	-0.013518
10 $r^3\sin(3t)$ (Trefoil 2)	0.35129
11 $(4r^2-3)r^2\cos(2t)$	-0.11499
12 $(4r^2-3)r^2\sin(2t)$	-0.015596
13 $(10r^4-12r^2+3)r\cos(t)$	0.0050869
14 $(10r^4-12r^2+3)r\sin(t)$	-0.11814
15 $20r^6-30r^4+12r^2-1$	0.016957
16 $r^4\cos(4t)$	0.15444
17 $r^4\sin(4t)$	0.02758
18 $(5r^2-4)r^3\cos(3t)$	-0.014778
19 $(5r^2-4)r^3\sin(3t)$	0.10097
20 $(15r^4-20r^2+6)r^2\cos(2t)$	-0.083978
21 $(15r^4-20r^2+6)r^2\sin(2t)$	-0.0076294
22 $(35r^6-60r^4+30r^2-4)r\cos(t)$	-0.0089318
23 $(35r^6-60r^4+30r^2-4)r\sin(t)$	-0.017889
24 $70r^8-140r^6+90r^4-20r^2+1$	0.014129
25 $r^5\cos(5t)$	0.026153
26 $r^5\sin(5t)$	-0.045199
27 $(6r^2-5)r^4\cos(4t)$	0.05774
28 $(6r^2-5)r^4\sin(4t)$	-0.0011454
29 $(21r^4-30r^2+10)r^3\cos(3t)$	0.0000731
30 $(21r^4-30r^2+10)r^3\sin(3t)$	0.0091797
31 $(56r^6-105r^4+60r^2-10)r^2\cos(2t)$	-0.02021
32 $(56r^6-105r^4+60r^2-10)r^2\sin(2t)$	-0.020879
33 $(126r^5-280r^6+210r^4-60r^2+5)r\cos(t)$	0.01269
34 $(126r^8-280r^6+210r^4-60r^2+5)r\sin(t)$	0.024791
35 $252r^{10}-630r^8+560r^6-210r^4+30r^2-1$	-0.035142
36 $r^6\cos(6t)$	-0.084566
37 $r^6\sin(6t)$	-0.019759
38 $(7r^2-6)r^5\cos(5t)$	0.011588
39 $(7r^2-6)r^5\sin(5t)$	-0.032458
40 $924r^{12}-2772r^{10}+3150r^8-1680r^6+420r^4-42r^2+1$	-0.019568
41 $r^7\cos(7t)$	-0.02198
42 $r^7\sin(7t)$	0.034523

Table 2. Zernikes for average ambient surface error profile (units are microns).

Zernike Term (ISO)	SBMD 2 AMB plus neg(35K-AMB)	SBMD 3 AMB
4 $r^2\cos(2t)$ (0 Astig)	1.009	1.041
5 $r^2\sin(2t)$ (45 Astig)	0.167	0.161
10 $r^3\sin(3t)$ (Trefoil 2)	0.309	0.351
16 $r^4\cos(4t)$	0.144	0.154

Table 3. Expected top 4 Zernikes vs. actual Zernikes (units are microns).

Vacuum & 38 K

Next, five independent measurements were made at vacuum and 38 K on September 5, 2000. Due to a lack of proper registration with the other measurements, the first cryo measurement (VAC-37K-2) was not used in any further data reduction. In Fig. 6 (next page), the upper plots show the average of the four remaining measurements, followed by the Zernike fit, and then the residual error. The PV & rms values for each case are given in Table 4.

Some high-frequency print-through can still be seen in the 38 K data. This was seen with the PDI also (see Fig. 7). A brief, manual comparison of the two residual plots indicated that some of the peaks & valleys from the ambient measurement did indeed disappear at cryo while others decreased only slightly and others actually got larger. The residual PV & rms values each decreased by about 27% from ambient. Also, the PSF was significantly smoother than that at ambient. No obvious dimple is seen at the center. The cryo-ambient difference will be discussed further below. The average radius of curvature at 38 K was 19.999 m.

Measurement	Pressure	Temperature	ROC	PV	rms
VAC/38K	1.3×10^{-5} Torr	37.87 K	19.999 m	2.403 μm	0.417 μm
Zernike Fit	"	"	N/A	2.040 μm	0.404 μm
Residual	"	"	N/A	0.145 μm	0.019 μm

Table 4. Summary of 38 K-average measurement results.

The Zernikes for the average 38 K surface are given in Table 5 below. The dominant terms, in order of magnitude, are 0° astigmatism, a 4θ term, trefoil (3θ), and Y coma. The 0° & 45° astigmatism terms are both a bit less than they were at ambient. The trefoil has gone down by a factor of two from ambient. The 4θ term & Y coma have increased slightly.

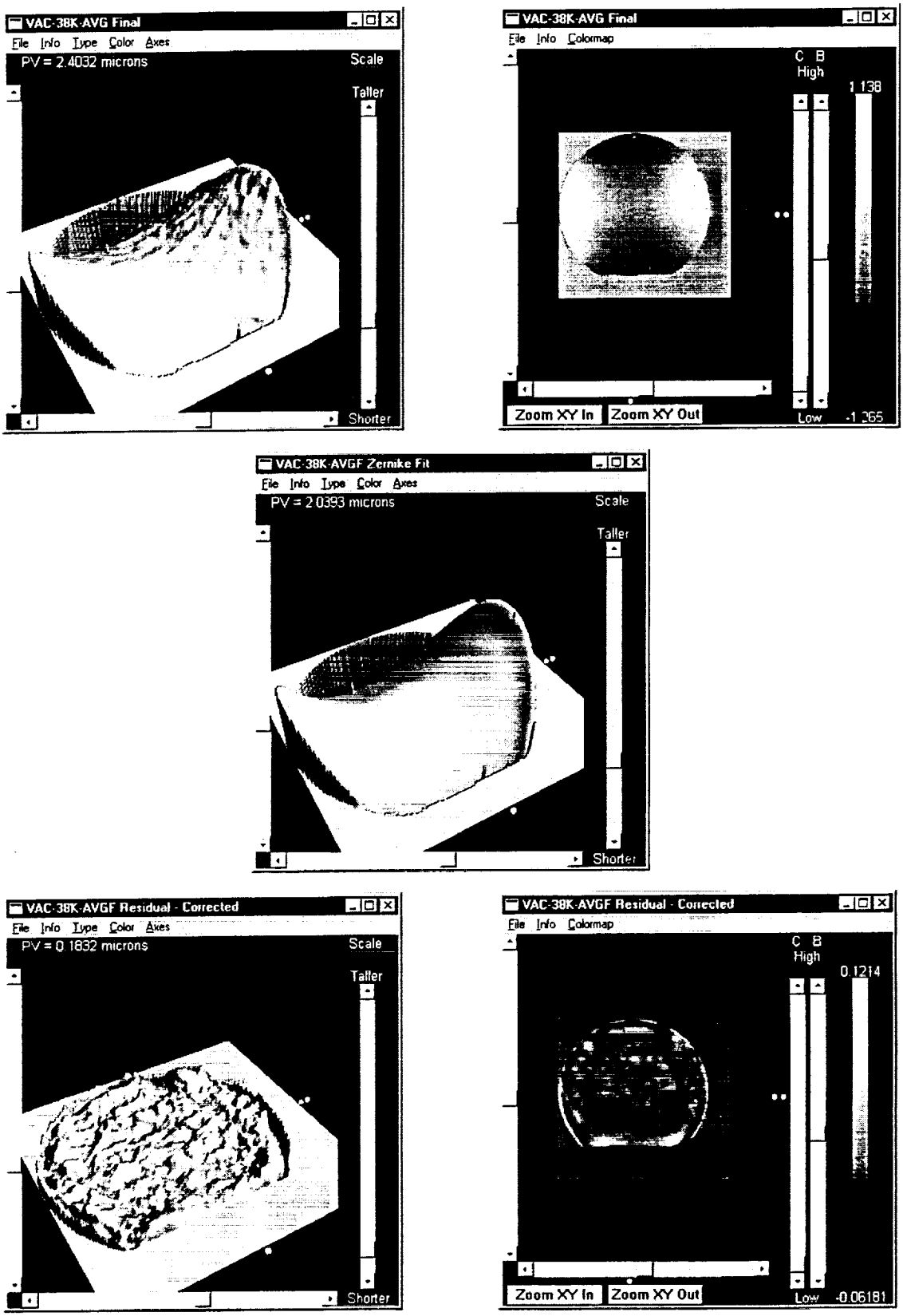

Figure 6. Average 38 K surface figure with Zernike decomposition and residual errors.

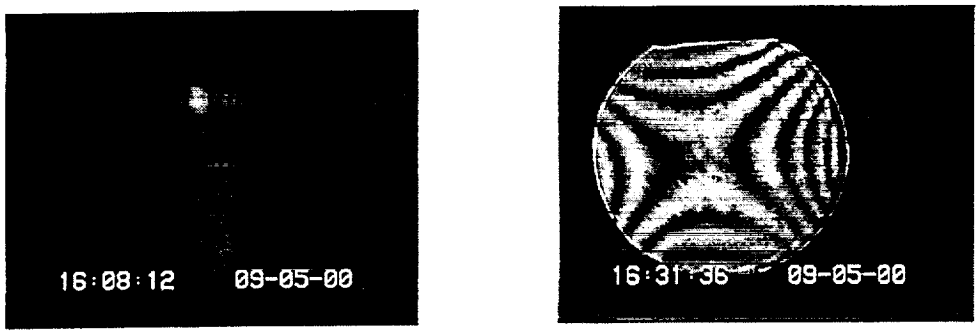

Figure 7. 38 K PSF (left) & PDI (right) results.

In Fig. 8 below, the upper plots show the difference between the average 38 K surface error and the average ambient surface error, followed by the Zernike fit, and then the residual error. The PV & rms values for the difference are given in Table 6. These values are slightly higher than those for the SBMD 2 cryo-ambient case; however, a smaller analysis pupil was used for the SBMD 2 test to mitigate edge effects. The top four Zernike terms for the difference are trefoil, 0° astigmatism, 45° astigmatism, & a 4θ term. The last two terms have switched places from the SBMD 2 test (all included in Table 5), but are relatively small. Overall, it seems that the cryo change has been quite repeatable between these tests.

Difference	PV	PV	rms	rms	Comments
VAC38KAVGF-VACAMBAVG	0.670 μm	λ/0.9	0.090 μm	λ/7.0	Mostly trefoil, dimple & print-thru.
Zernike Fit	0.617 μm	λ/1.0	0.086 μm	λ/7.4	No print-thru.
Residual	0.166 μm	λ/3.8	0.016 μm	λ/40	Triangular print-thru.

Table 6. Summary of 38 K minus AMB results.

Zernike Term (ISO)	38K, AVG	38K-AMB	34K-AMB (Test 2)
0 1.0 (Piston)	0.0022016	0.0002982	0.0009579
1 rcos(t) (X Tilt)	0.038797	0.022592	0.024778
2 rsin(t) (Y Tilt)	-0.0022544	0.021914	0.0009471
3 $2r^2-1$ (Focus)	0.059286	0.0016294	0.0052838
4 $r^2\cos(2t)$ (0 Astig)	0.9187	-0.12702	-0.10497
5 $r^2\sin(2t)$ (45 Astig)	0.11826	-0.044219	-0.022901
6 $(3r^2-2)r\cos(t)$ (X Coma)	0.0050555	-0.0095757	0.0070569
7 $(3r^2-2)r\sin(t)$ (Y Coma)	-0.14977	-0.026671	-0.012151
8 $6r^4-6r^2+1$ (Spherical)	0.062144	-0.018393	-0.021015
9 $r^3\cos(3t)$ (Trefoil 1)	-0.0077763	0.0014693	-0.0053622
10 $r^3\sin(3t)$ (Trefoil 2)	0.18234	-0.16483	-0.16503
11 $(4r^2-3)r^2\cos(2t)$	-0.12431	-0.01185	-0.0097391
12 $(4r^2-3)r^2\sin(2t)$	-0.011748	0.0040602	0.0022686
13 $(10r^4-12r^2+3)r\cos(t)$	-0.0053936	-0.01342	-0.0095831
14 $(10r^4-12r^2+3)r\sin(t)$	-0.099587	0.022343	0.016065
15 $20r^6-30r^4+12r^2-1$	0.032901	0.011957	0.016040
16 $r^4\cos(4t)$	0.19061	0.039635	0.042163
17 $r^4\sin(4t)$	0.0030675	-0.017794	-0.013380
18 $(5r^2-4)r^3\cos(3t)$	-0.0091933	0.0037996	0.0073302
19 $(5r^2-4)r^3\sin(3t)$	0.096265	-0.0048648	-0.0042847
20 $(15r^4-20r^2+6)r^2\cos(2t)$	-0.076497	0.0088803	0.0014423
21 $(15r^4-20r^2+6)r^2\sin(2t)$	-0.014689	-0.0038161	-0.0087684
22 $(35r^6-60r^4+30r^2-4)r\cos(t)$	0.0038399	0.0074886	0.0097362
23 $(35r^6-60r^4+30r^2-4)r\sin(t)$	-0.032889	-0.0086314	-0.0078693
24 $70r^8-140r^6+90r^4-20r^2+1$	-0.0078097	-0.02605	-0.020375
25 $r^5\cos(5t)$	0.0065809	-0.012012	-0.0073614
26 $r^5\sin(5t)$	-0.056795	-0.014556	-0.018153
27 $(6r^2-5)r^4\cos(4t)$	0.054956	-0.0052666	-0.0049222
28 $(6r^2-5)r^4\sin(4t)$	0.0020141	0.0051825	0.0032922
29 $(21r^4-30r^2+10)r^3\cos(3t)$	-0.0052701	-0.0036387	-0.0031708
30 $(21r^4-30r^2+10)r^3\sin(3t)$	0.025831	0.013172	0.010089
31 $(56r^6-105r^4+60r^2-10)r^2\cos(2t)$	-0.020966	0.0011352	0.0063532
32 $(56r^6-105r^4+60r^2-10)r^2\sin(2t)$	-0.011287	0.015268	0.0091755
33 $(126r^8-280r^6+210r^4-60r^2+5)r\cos(t)$	0.0036584	-0.015618	-0.015806
34 $(126r^8-280r^6+210r^4-60r^2+5)r\sin(t)$	0.028406	0.0067164	0.0045368
35 $252r^{10}-630r^8+560r^6-210r^4+30r^2-1$	-0.021169	0.012168	0.0068764
36 $r^6\cos(6t)$	-0.070523	0.0096498	0.018749
37 $r^6\sin(6t)$	-0.016971	-0.0046146	0.0008569
38 $(7r^2-6)r^5\cos(5t)$	0.0084666	-0.0026928	-0.0026386
39 $(7r^2-6)r^5\sin(5t)$	-0.037217	-0.001528	-0.0022646
40 $924r^{12}-2772r^{10}+3150r^8-1680r^6+420r^4-42r^2+1$	-0.027756	-0.0072171	-0.0028693
41 $r^7\cos(7t)$	-0.0072495	0.010004	0.012247
42 $r^7\sin(7t)$	0.033646	-0.0009763	0.010215

Table 5. Zernikes for average 38 K & 38K-AMB surface error profile (units are microns).

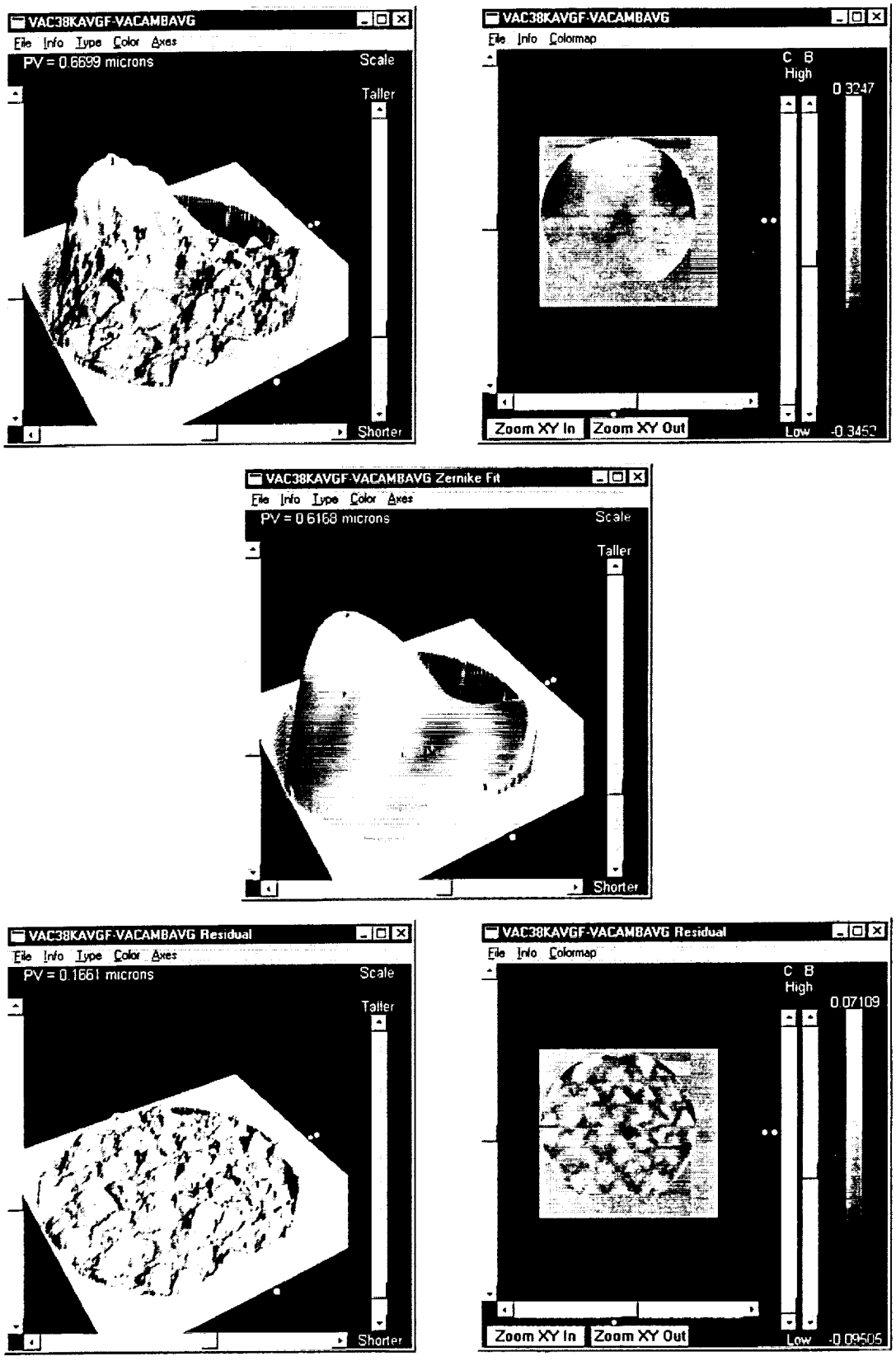

Figure 8. 38K-AMB surface difference with Zernike decomposition and residual errors.

Vacuum & 46 K

A single measurement was made at vacuum and 46 K on September 6, 2000 with a reverse axial gradient induced in the mirror assembly. During the 38 K measurements, the average axial gradient (facesheet – backsheet) was –3.69 K (i.e. facesheet colder). For this measurement, a small heater located between the facesheet & backsheet and facing the facesheet was used to reverse the gradient to 1.39 K (i.e. facesheet hotter). Thus, the change in the axial gradient between the 38 K measurements and this 46 K measurement was 5.08 K. The entire mirror assembly warmed up during heater operation, causing the 46 K temperature. The raw rms differed from the 38 K average by only λ/70. The PV & rms values for the point-by-point difference between the average 38 K surface error and the single 46 K surface error are given in Table 7. The top four Zernike terms for the difference are 45° astigmatism, X tilt, Y tilt, & X coma. Due to the fact that the 46 K measurement was not the usual average of five, the dominance of 45° astigmatism & tilt, previously associated with measurement errors and plot mis-registration, is not surprising. If these are ignored, then one sees very little change in the low-order figure with the gradient change. Also, the high-frequency change is on the order of the measurement noise. Thus, it seems that the change in axial gradient of 5.08 K had little effect on the mirror shape.

Difference	PV	PV	rms	rms	Comments
VAC38KAVGF-VAC46K2	0.243 μm	λ/2.6	0.047 μm	λ/14	Mostly 45° astig & tilt.
Zernike Fit	0.194 μm	λ/3.3	0.045 μm	λ/14	Small chg in dimple.
Residual	0.059 μm	λ/11	0.008 μm	λ/79	Looks like noise.

Table 7. Summary of 38 K minus 46 K results.

Vacuum & 99 K

Next, five independent measurements were made at vacuum and 99 K on September 10, 2000. Due to a lack of proper registration with the other measurements, the first measurement (VAC-98K-2) was not used in any further data reduction. The remaining four measurements were averaged, and a Zernike fit and residual error analysis was conducted. The Peak-to-Valley (PV) & rms values for each case are given in Table 8. Due to the almost identical look of the resulting plots, they are not included here.

Looking at the two average surfaces, the 99 K results look very similar to the 38 K results. The PSF & PDI data also look quite similar. The PV's differ by an average of only λ/19, while the rms's differ by an average of λ/475. Meanwhile, the average radius of curvature at 99 K was down a little from the 38 K case to 19.996 m (the difference is within the accuracy of the measurement).

Measurement	Pressure	Temperature	ROC	PV	rms
VAC/99K	$1.0x10^{-5}$ Torr	98.64 K	19.996 m	2.431 μm	0.417 μm
Zernike Fit	"	"	N/A	2.072 μm	0.404 μm
Residual	"	"	N/A	0.145 μm	0.020 μm

Table 8. Summary of 99 K-average measurement results.

The Zernikes for the average 99 K surface are given in Table 9 (next page). The dominant terms, in order of magnitude, are 0° astigmatism, trefoil (3θ), 45° astigmatism, and a 4θ term. The 0° astigmatism, the 4θ term, and the Y coma are all slightly lower than at 38 K, while the trefoil and 45° astigmatism are higher.

In Fig. 9, the upper plots show the difference between the average 38 K surface error and the average 99 K surface error, followed by the Zernike fit, and then the residual error. The PV & rms values for the difference are given in Table 10. The top four Zernike terms for the difference (see Table 9) are 45° astigmatism, X tilt, trefoil, & Y tilt. Despite using averaging for both measurements, the dominance of 45° astigmatism & tilt again indicate the possibility of measurement errors and plot mis-registration in this difference. Irregardless of these, one still sees a change in the trefoil as well as depressions at the titanium attachment points (visible in the raw, Zernike, & residual plots). The axial gradient for the 99 K measurement was only 0.52 K and should not be a factor. Aside from the attachment points, there seemed to be no significant change in the high-frequency print-through. In summary, it would be difficult, although not impossible, to conclude at this point that measurements of this mirror at 100 K are essentially equivalent to measurements at 35 K.

Difference	PV	PV	rms	Rms	Comments
VAC38KAVGF-VAC99KAVGF	0.282 μm	λ/2.2	0.053 μm	λ/12	Mostly 45° astig & trefoil, & bumps.
Zernike Fit	0.249 μm	λ/2.5	0.051 μm	λ/12	Small chg in dimple.
Residual	0.067 μm	λ/9.4	0.009 μm	λ/70	Mostly noise.

Table 10. Summary of 38 K minus 99 K results.

Zernike Term (ISO)	99K, AVG	38K-99K
0 1.0 (Piston)	0.0027508	0.0007972
1 rcos(t) (X Tilt)	-0.022968	0.062281
2 rsin(t) (Y Tilt)	-0.03673	0.030663
3 $2r^2-1$ (Focus)	0.062728	-0.0009558
4 $r^2\cos(2t)$ (0 Astig)	0.90668	0.0063581
5 $r^2\sin(2t)$ (45 Astig)	0.18274	-0.066807
6 $(3r^2-2)r\cos(t)$ (X Coma)	0.033547	-0.028162
7 $(3r^2-2)r\sin(t)$ (Y Coma)	-0.12471	-0.027544
8 $6r^4-6r^2+1$ (Spherical)	0.057709	0.005031
9 $r^3\cos(3t)$ (Trefoil 1)	-0.024432	0.011197
10 $r^3\sin(3t)$ (Trefoil 2)	0.23099	-0.044385
11 $(4r^2-3)r^2\cos(2t)$	-0.10549	-0.020677
12 $(4r^2-3)r^2\sin(2t)$	-0.021583	0.0080309
13 $(10r^4-12r^2+3)r\cos(t)$	0.0075344	-0.013858
14 $(10r^4-12r^2+3)r\sin(t)$	-0.09005	-0.0060469
15 $20r^6-30r^4+12r^2-1$	0.036699	-0.0062923
16 $r^4\cos(4t)$	0.17418	0.021814
17 $r^4\sin(4t)$	0.018751	-0.0077272
18 $(5r^2-4)r^3\cos(3t)$	-0.017324	0.0037507
19 $(5r^2-4)r^3\sin(3t)$	0.090979	0.0032085
20 $(15r^4-20r^2+6)r^2\cos(2t)$	-0.065853	-0.0058279
21 $(15r^4-20r^2+6)r^2\sin(2t)$	-0.017336	0.003446
22 $(35r^6-60r^4+30r^2-4)r\cos(t)$	0.0053319	-0.0044495
23 $(35r^6-60r^4+30r^2-4)r\sin(t)$	-0.022132	-0.0028214
24 $70r^8-140r^6+90r^4-20r^2+1$	-0.0081343	-0.0030015
25 $r^5\cos(5t)$	0.019695	-0.0063029
26 $r^5\sin(5t)$	-0.04759	-0.011271
27 $(6r^2-5)r^4\cos(4t)$	0.042841	0.009851
28 $(6r^2-5)r^4\sin(4t)$	0.011553	-0.0037034
29 $(21r^4-30r^2+10)r^3\cos(3t)$	-0.0097101	0.0037152
30 $(21r^4-30r^2+10)r^3\sin(3t)$	0.0076602	0.010541
31 $(56r^6-105r^4+60r^2-10)r^2\cos(2t)$	-0.017227	0.0035106
32 $(56r^6-105r^4+60r^2-10)r^2\sin(2t)$	-0.014536	0.0075292
33 $(126r^8-280r^6+210r^4-60r^2+5)r\cos(t)$	0.0022445	-0.0033537
34 $(126r^8-280r^6+210r^4-60r^2+5)r\sin(t)$	0.02947	0.0040055
35 $252r^{10}-630r^8+560r^6-210r^4+30r^2-1$	-0.020842	-0.000741
36 $r^6\cos(6t)$	-0.074856	0.0011879
37 $r^6\sin(6t)$	-0.025336	0.005689
38 $(7r^2-6)r^5\cos(5t)$	0.012735	-0.0006722
39 $(7r^2-6)r^5\sin(5t)$	-0.028493	-0.0030406
40 $924r^{12}-2772r^{10}+3150r^8-1680r^6+420r^4-42r^2+1$	-0.018836	-0.0050953
41 $r^7\cos(7t)$	-0.0086847	0.0036273
42 $r^7\sin(7t)$	0.028836	0.004935

Table 9. Zernikes for average 99 K & 38K-99K surface error profiles (units are microns).

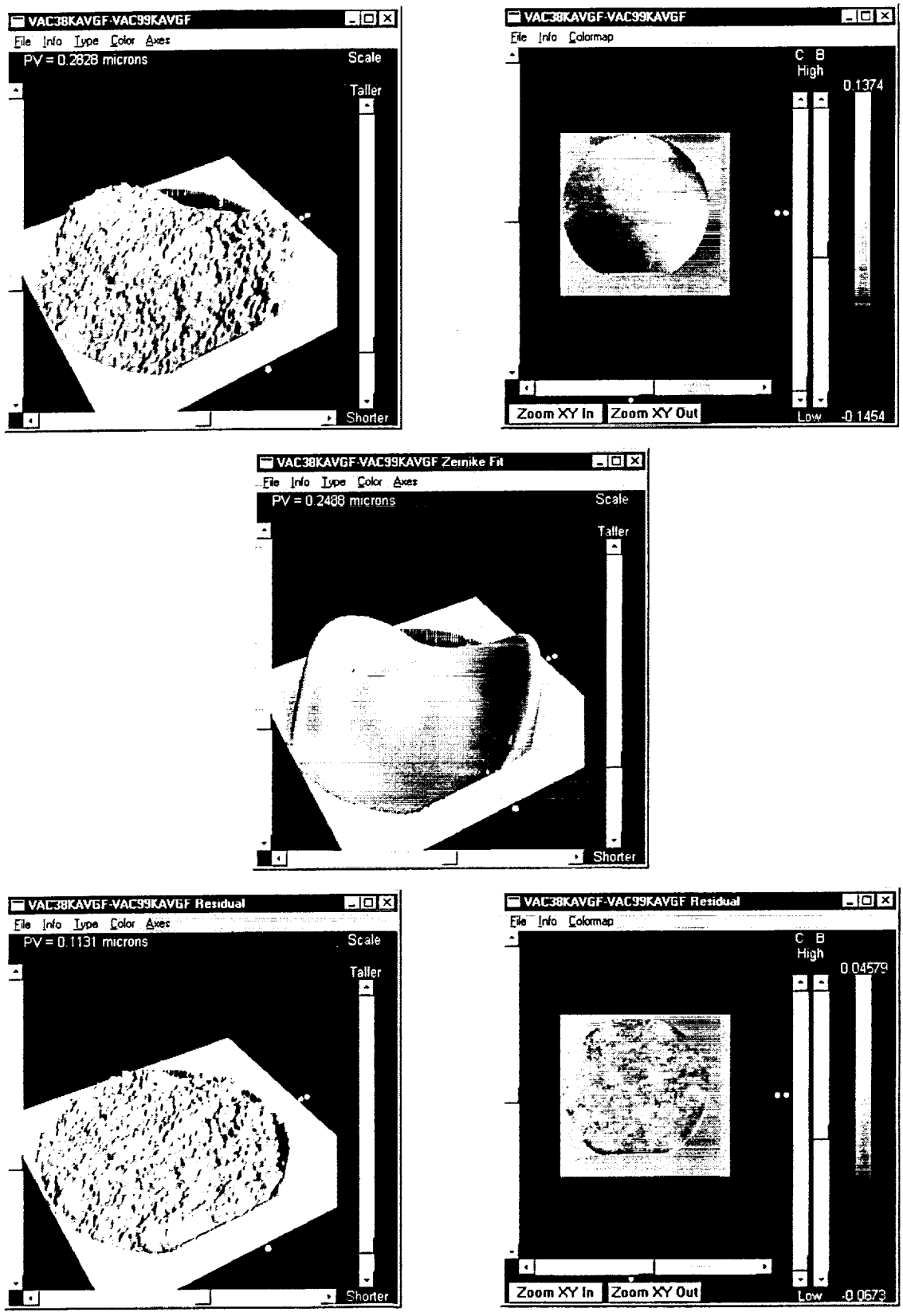

Figure 9. 38K-99K surface difference with Zernike decomposition and residual errors.

Vacuum & Ambient Temperature #2

Five independent measurements were made at vacuum and ambient temperature following the cryo measurements on September 17, 2000. As with the 38 K case, a lack of proper registration was noticed for two of these measurements (VAC-296Kb-2 & VAC-296Kĉ-2). Thus, these measurements were not used in any further data reduction. The remaining three measurements were averaged, and a Zernike fit and residual error analysis was conducted. The PV & rms values for each case are given in Table 11. Due to the almost identical look of the resulting plots to the pre-cryo, ambient results, they are not included here. Meanwhile, the average radius of curvature was up a little from the pre-cryo case to 20.020 m (the difference is within the accuracy of the measurement).

Measurement	Pressure	Temperature	ROC	PV	rms
VAC/AMB2	2.0×10^{-4} Torr	292.10 K	20.020 m	3.051 μm	0.484 μm
Zernike Fit	"	"	N/A	2.535 μm	0.471 μm
Residual	"	"	N/A	0.191 μm	0.027 μm

Table 11. Summary of post-cryo, ambient-average measurement results.

The Zernikes for the average surface are given in Table 12 (next page). The dominant terms, in order of magnitude, are 0° astigmatism, trefoil (3θ), a 4θ term, and 45° astigmatism. Just as with the 38 K case, the last two terms have switched places with respect to the pre-cryo case, suggesting a permanent change.

In Fig. 10, the upper plots show the difference between the post-cryo average surface error and the pre-cryo average surface error, followed by the Zernike fit, and then the residual error. The PV & rms values for the difference are given in Table 13. The values in the table have been corrected for noise spikes in the data and may differ from the PV values shown on the figure plots. The most interesting feature is a very noticeable indentation near the 1 o'clock position. It seems to be too far away from the Si diode clamp for that to have been a possible cause. It does correspond to the position of one of the bipod attach points; but, it is not obvious why only one such point would end up with a permanent distortion. The indent shows up in the raw data, the Zernike fit, and the residual. Without the indent, all of the PV's below would be less than λ/10. The top five Zernike terms for the difference (see Table 12) are 45° astigmatism, 0° astigmatism, both trefoil terms, & Y tilt. The tilt indicates some small mis-registration in the difference.

Difference	PV	PV	rms	rms	Comments
VACAMB2AVGF -VACAMBAVG	0.127 μm	λ/5.0	0.017 μm	λ/37	Mostly 0° & 45° astig w/ indent.
Zernike Fit	0.105 μm	λ/6.0	0.015 μm	λ/42	
Residual	0.053 μm	λ/12	0.006 μm	λ/106	Mostly noise.

Table 13. Summary of post-cryo minus pre-cryo ambient results.

Zernike Term (ISO)	AMB2, AVG	AMB2-AMB
0 1.0 (Piston)	0.002584	0.0001692
1 rcos(t) (X Tilt)	0.01834	0.0031389
2 rsin(t) (Y Tilt)	-0.032881	-0.0070356
3 $2r^2-1$ (Focus)	0.058257	0.0000276
4 $r^2\cos(2t)$ (0 Astig)	1.0600	0.017559
5 $r^2\sin(2t)$ (45 Astig)	0.13767	-0.026085
6 $(3r^2-2)r\cos(t)$ (X Coma)	0.0060359	-0.0068324
7 $(3r^2-2)r\sin(t)$ (Y Coma)	-0.12906	-0.0055929
8 $6r^4-6r^2+1$ (Spherical)	0.083996	0.0043532
9 $r^3\cos(3t)$ (Trefoil 1)	-0.0002354	0.0079807
10 $r^3\sin(3t)$ (Trefoil 2)	0.34261	-0.0073658
11 $(4r^2-3)r^2\cos(2t)$	-0.11768	-0.0042358
12 $(4r^2-3)r^2\sin(2t)$	-0.010257	0.0042562
13 $(10r^4-12r^2+3)r\cos(t)$	0.0059283	-0.0000216
14 $(10r^4-12r^2+3)r\sin(t)$	-0.12042	-0.0016577
15 $20r^6-30r^4+12r^2-1$	0.016632	-0.0013644
16 $r^4\cos(4t)$	0.15643	0.0008825
17 $r^4\sin(4t)$	0.016741	-0.0028488
18 $(5r^2-4)r^3\cos(3t)$	-0.013225	-0.0005000
19 $(5r^2-4)r^3\sin(3t)$	0.10662	0.0065663
20 $(15r^4-20r^2+6)r^2\cos(2t)$	-0.084151	-0.0014283
21 $(15r^4-20r^2+6)r^2\sin(2t)$	-0.010567	-0.0005103
22 $(35r^6-60r^4+30r^2-4)r\cos(t)$	-0.0085678	-0.0026888
23 $(35r^6-60r^4+30r^2-4)r\sin(t)$	-0.016922	0.0018207
24 $70r^8-140r^6+90r^4-20r^2+1$	0.015448	0.0004299
25 $r^5\cos(5t)$	0.012588	-0.0055632
26 $r^5\sin(5t)$	-0.044049	0.0029041
27 $(6r^2-5)r^4\cos(4t)$	0.060704	0.0007681
28 $(6r^2-5)r^4\sin(4t)$	-0.0001120	0.002938
29 $(21r^4-30r^2+10)r^3\cos(3t)$	-0.0015176	0.0009870
30 $(21r^4-30r^2+10)r^3\sin(3t)$	0.0082755	-0.0000167
31 $(56r^6-105r^4+60r^2-10)r^2\cos(2t)$	-0.018734	-0.0001209
32 $(56r^6-105r^4+60r^2-10)r^2\sin(2t)$	-0.02364	0.0024493
33 $(126r^8-280r^6+210r^4-60r^2+5)r\cos(t)$	0.01878	0.0017417
34 $(126r^8-280r^6+210r^4-60r^2+5)r\sin(t)$	0.024679	-0.0000003
35 $252r^{10}-630r^8+560r^6-210r^4+30r^2-1$	-0.036035	-0.0012128
36 $r^6\cos(6t)$	-0.091202	-0.0069053
37 $r^6\sin(6t)$	-0.012618	0.000322
38 $(7r^2-6)r^5\cos(5t)$	0.01537	0.0023523
39 $(7r^2-6)r^5\sin(5t)$	-0.034734	0.0007709
40 $924r^{12}-2772r^{10}+3150r^8-1680r^6+420r^4-42r^2+1$	-0.022596	-0.0029782
41 $r^7\cos(7t)$	-0.017061	-0.001397
42 $r^7\sin(7t)$	0.033264	-0.0018327

Table 12. Zernikes for average post-cryo ambient & post-pre difference surface error profiles (units are microns).

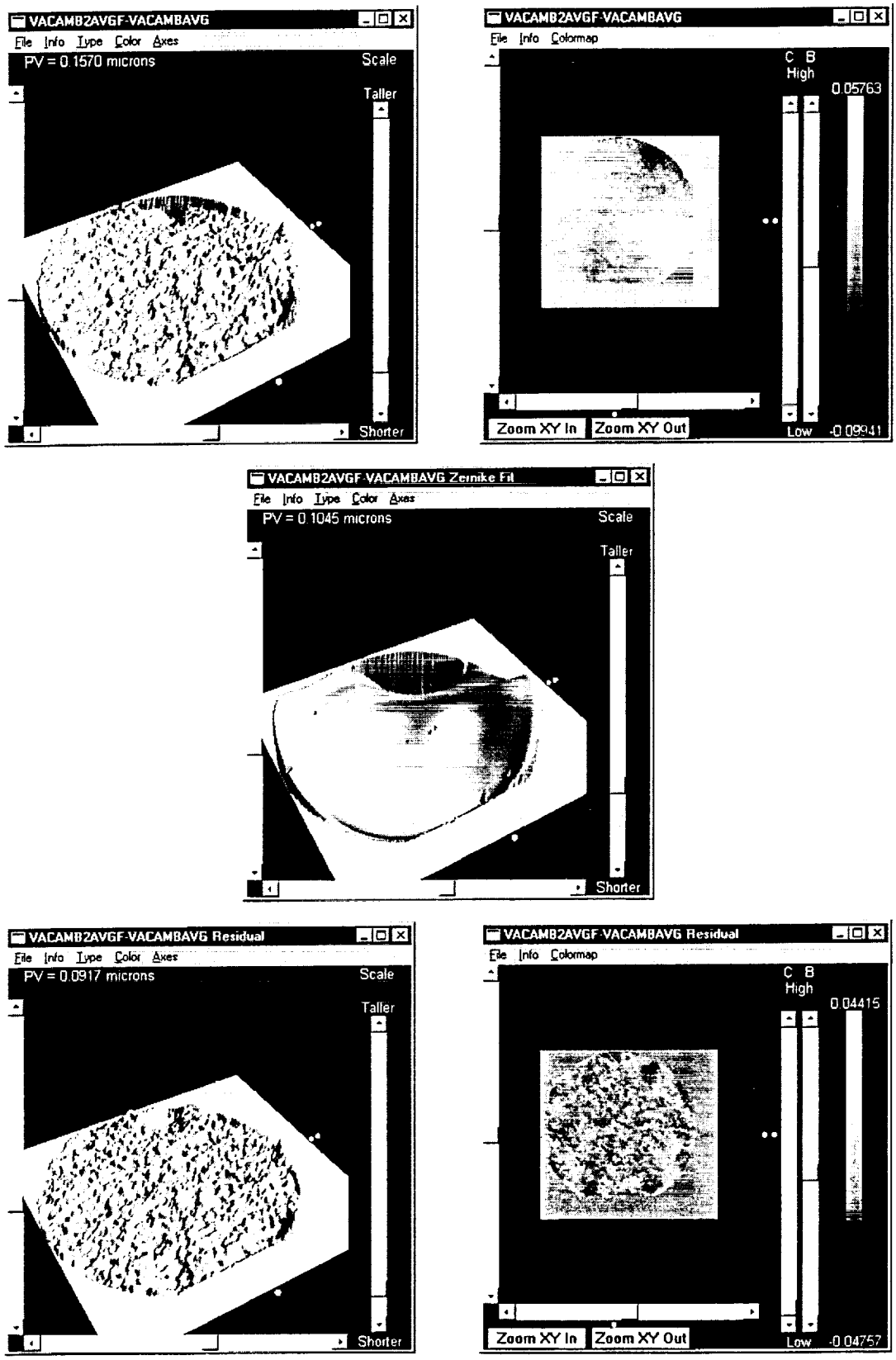

Figure 10. Post, pre-cryo ambient surface difference with Zernike decomposition and residual errors.

Ambient Pressure & Temperature #2

Measurements in six orientations at ambient pressure & temperature were made on September 18 & 19, 2000. The data was sent to SVG-Tinsley for averaging. The post-cryo average was within 15 nm rms of the pre-cryo average.

5.0 Final Cryogenic Figure

The question now becomes, what is the G-corrected figure at cryo? One way to calculate this is to apply the 38K-AMB difference shown above to the average of the six rotations done at ambient. This was done by SVG/Tinsley. The result for a 500 mm diameter analysis circle is shown in Fig. 11. The PV is 0.109 μm or λ/5.8. This meets the requirement of λ/4. The rms is 0.0174 μm or λ/36. The error consists of trefoil, coma, astigmatism, and some residual print-through.

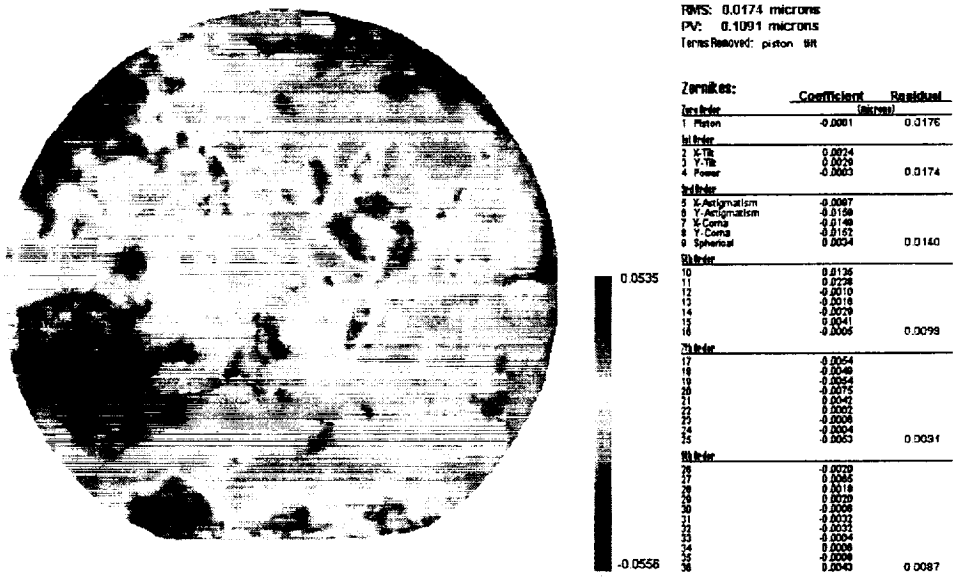

Figure 11. Final SBMD cryogenic figure error.

A Power Spectral Density (PSD) analysis was carried out to quantify the mid-spatial (1-10 cm spatial wavelength or 0.01-0.1 cyc/mm) figure error from the ambient & cryo measurements made during SBMD tests 2 & 3. This would indicate how well the high-frequency errors were corrected by cryo-figuring as a function of spatial frequency.

The analysis started with the "residual" surface error results (i.e. raw results minus 42 term Zernike fit) in order to eliminate most of the low-order errors. The WaveScope atomic commands were used to calculate the PSD. The FFT command required a $2^n x 2^n$ array. Thus, the original 150x150 residual arrays were cut down to 64x64 arrays centered on the mirror. This

avoided any edge effects while providing a good sampling of the high-frequency print-through. The PSD was calculated using the following equation.

$$PSD(f_i,f_j) = (d/N)^2 \, |\mathcal{FF}[SE(n,m)]|^2$$

In the equation, d = point spacing of SE (3550.5 μm), N = # of points on a side for square array (64), SE(n,m) = surface error at point n,m in μm, $f_{i/j}$ = spat freq where $\Delta f_{i/j}$ = 1/Nd (0.0044 cyc/mm), where i/j vary from 1 to N/2 & d is in mm. The units for this 2-D PSD are μm^4.

The PSD results were then imported into Excel for plotting and calculation of the mid-spatial rms's & estimated PV's. The mid-spatial frequency rms for each case was calculated by integrating the 2-D PSD between 0.01 & 0.1 cyc/mm, corresponding to the defined range of 1-10 cm spatial wavelengths. In general, these values were near the full rms values where the PSD was integrated over the full range of spatial frequencies (0.0044-0.1408 cyc/mm). This is because the low-frequency errors had already been removed by the Zernike fit subtraction. The mid-spatial PV's were estimated by multiplying each mid-spatial rms by the corresponding PV/rms ratio for the full spatial frequency case (using numbers from the WaveScope). The full rms values calculated from the PSD's always matched the WaveScope values exactly. So, the mid-spatial rms's should be nearly as accurate, along with the estimated PV's. The results are given in Fig. 12 and Table 14 below. 2-D slices of the 3-D PSD's in the row direction are given in the figures.

CASE	MID-SPATIAL ERROR (nm)	
	PV	rms
SBMD 2 AMB	36	5
SBMD 2 34 K	94	15
SBMD 2 CHG	+58	+10
SBMD 3 AMB	90	14
SBMD 3 38 K	57	9
SBMD 3 CHG	-33	-5

Table 14. Mid-spatial error results from PSD analysis for SBMD cryo tests 2 & 3.

The SBMD 2 results show a three-fold increase in mid-spatial error at cryo lying in the 0.01-0.03 cyc/mm (5-16 cyc/diam) range. The peaks in the row & column directions correspond well to the back-side triangle scales. The SBMD 3 ambient results show good correlation to the SBMD 2 cryo results. However, the mid-spatial errors at cryo are only corrected by about 50% with respect to ambient. The correction seems to be very effective in the 0.013-0.020 cyc/mm (7-11 cyc/diam) range, but not as effective above or below. However, the estimated mid-spatial PV of λ/11 meets the required λ/10. These results agree with the λ/10 value calculated by Ball using a subaperture analysis.

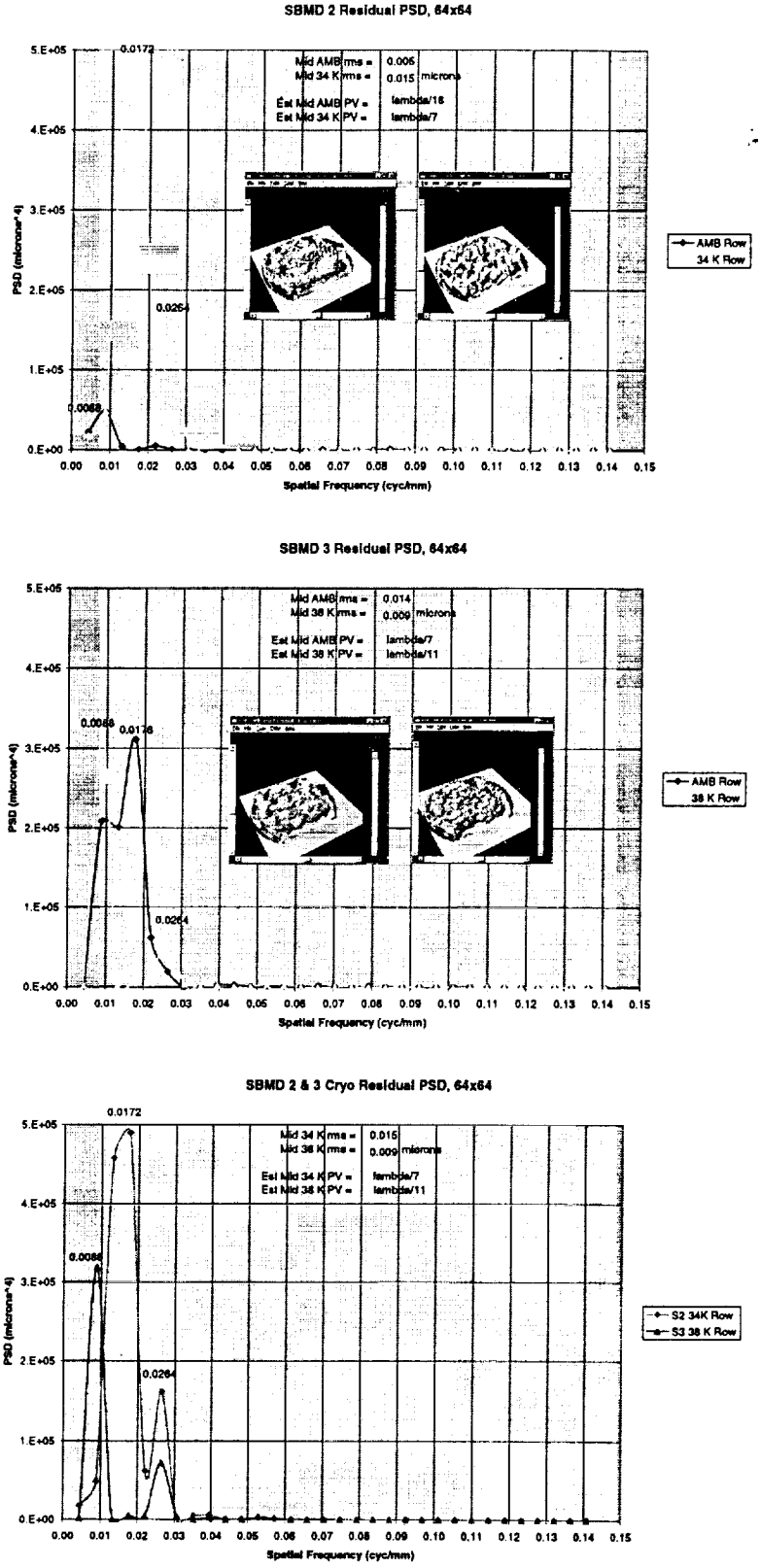

Figure 12. PSD results for SBMD cryo tests 2 & 3.

6.0 Conclusions

This cryogenic test of the SBMD verified that the requirements of figure error $\leq\lambda/4$ PV, mid-spatial error (surface wavelengths 1-10 cm) $\leq\lambda/10$ PV, and radius of curvature of 20.0±0.1 m at 35±5 K had been met. The metrology instrumentation and procedures developed in earlier tests provided the measurements and accuracies needed with no anomalies.

REPORT DOCUMENTATION PAGE

Form Approved
OMB No. 0704-0188

1. AGENCY USE ONLY *(Leave blank)*	2. REPORT DATE	3. REPORT TYPE AND DATES COVERED
	June 29, 2001	Final

4. TITLE AND SUBTITLE
Subscale Beryllium Mirror Demonstrator Testing Support

5. FUNDING NUMBERS
H-33241D

6. AUTHOR(S)
James B. Hadaway, Patrick Reardon, Joseph Geary, & Bruce Peters

7. PERFORMING ORGANIZATION NAME(S) AND ADDRESS(ES)
Univ of Alabama in Huntsville
301 Sparkman Dr.
Huntsville, AL 35899

8. PERFORMING ORGANIZATION REPORT NUMBER
521134-FR

9. SPONSORING/MONITORING AGENCY NAME(S) AND ADDRESS(ES)
NASA/MSFC
Huntsville, AL

10. SPONSORING/MONITORING AGENCY REPORT NUMBER

11. SUPPLEMENTARY NOTES

12a. DISTRIBUTION AVAILABILITY STATEMENT

12b. DISTRIBUTION CODE

13. ABSTRACT *(Maximum 200 words)*

This report details the tasks completed by UAH in support of MSFCs third cryogenic test of the Subscale Beryllium Mirror Demonstrator (SBMD) at the X-Ray Calibration Facility (XRCF).

14. SUBJECT TERMS
optical testing, cryogenic, beryllium

15. NUMBER OF PAGES
24

16. PRICE CODE

17. SECURITY CLASSIFICATION OF REPORT	18. SECURITY CLASSIFICATION OF THIS PAGE	19. SECURITY CLASSIFICATION OF ABSTRACT	20. LIMITATION OF ABSTRACT